Baghdad Science Journal

Volume 22 | Issue 6 Article 10

6-17-2025

Photocatalytic Degradation of Acid Yellow 25 Using Nanoparticle TiO_2 Mediated Petai Pod Extract

Anthoni Batahan Aritonang
Chemistry Department, Natural Science and Math, Tanjungpura University, Pontianak, Indonesia, anthoni.b.aritonang@chemistry.untan.ac.id

Reza Audina Putri
Research Centre for Chemistry, National Research and Innovation Agency, Serpong, Indonesia, rezaaudina002@gmail.com

Vivi Sisca
Research Centre for Chemistry, National Research and Innovation Agency, Serpong, Indonesia, vivi009@brin.go.id

Mohammad Jihad Madiabu
Department of Analytical Chemistry, Politeknik AKA Bogor, Bogor, Indonesia, mjihad1991@gmail.com

Khoiriah Khoiriah
Research Centre for Chemistry, National Research and Innovation Agency, Serpong, Indonesia, khoi013@brin.go.id

How to Cite this Article

Aritonang, Anthoni Batahan; Putri, Reza Audina; Sisca, Vivi; Madiabu, Mohammad Jihad; and Khoiriah, Khoiriah (2025) "Photocatalytic Degradation of Acid Yellow 25 Using Nanoparticle TiO_2 Mediated Petai Pod Extract," *Baghdad Science Journal*: Vol. 22: Iss. 6, Article 10.
DOI: https://doi.org/10.21123/2411-7986.4960

BAGHDAD SCIENCE JOURNAL 2025;22(6):1851–1862

Scan the QR to view the full-text article on the journal website

RESEARCH ARTICLE

Photocatalytic Degradation of Acid Yellow 25 Using Nanoparticle TiO_2 Mediated Petai Pod Extract

Anthoni Batahan Aritonang [1], Reza Audina Putri [2], Vivi Sisca [2], Mohammad Jihad Madiabu [3], Khoiriah Khoiriah [2,*]

[1] Chemistry Department, Natural Science and Math, Tanjungpura University, Pontianak, Indonesia
[2] Research Centre for Chemistry, National Research and Innovation Agency, Serpong, Indonesia
[3] Department of Analytical Chemistry, Politeknik AKA Bogor, Bogor, Indonesia

ABSTRACT

Nanotechnology has significant advantages over traditional methods for degrading dyes. Plant-based nanoparticles were generated apart from other biomaterials. This work employed a green sol-gel approach to prepare titanium dioxide nanoparticles by using Petai (*Parkia speciosa*) peel extract. The produced TiO_2 was analyzed by XRD, UV-DRS, FE-SEM, FTIR, Raman, zeta, and nanoparticle size analysis. PP-TiO_2 nanoparticles having a tetragonal anatase phase, spherical, stable particles, and a small particle size (16–22 nm) were successfully produced. When exposed to UV light, the nanoparticles displayed strong photocatalytic activity, eliminating Acid Yellow 25 in less than 120 minutes. This work demonstrates a possible green option to sustainable wastewater treatment based on TiO_2 NPs.

Keywords: Green strategies, Nanoparticles, Petai, Photocatalyst, Titanium dioxide

Introduction

Nanobiotechnology is an emerging topic of study that focuses on the role of biological species in the development of synthetic nanomaterials and nanocomposites. Nanomaterials are materials with a size of less than 100 nm in at least one dimension. [1] Nano-sized materials differ from bulk-sized materials in terms of physical, chemical, electrical, mechanical, and optical properties due to their small size, huge surface area, and high surface activity. [2]

Titanium dioxide (TiO_2) is a solid transition metal oxide that is both common and environmentally acceptable due to its non-toxicity and lack of flammability. TiO_2 is also chemically and thermally stable, with excellent corrosion and oxidation resistance. TiO_2 is an excellent semiconductor, and the three naturally occurring crystalline forms of TiO_2 are rutile, anatase, and brookite, which have band gap energies of 3.0, 3.2, and 2.96 eV, respectively. [3] Anatase and rutile have tetragonal structures with distinct space groups. Brookite, on the other hand, has an orthogonal structure. Rutile is the most stable phase, but anatase and brookite are metastable phases that can be converted to rutile when heated. Anatase is the most electrochemically active phase due to its crystalline structure. [3]

TiO_2 nanoparticles (TNPs) exhibit excellent optical characteristics. TNP is widely utilized as a photocatalyst, an antibacterial agent, and an electrode material in energy storage devices such lithium-ion batteries and supercapacitors. [4–6] TiO_2 NPs have been synthesized using a variety of physical and chemical processes, including ball milling, microwave

Received 8 May 2024; revised 24 August 2024; accepted 26 August 2024.
Available online 17 June 2025

* Corresponding author.
E-mail addresses: anthoni.b.aritonang@chemistry.untan.ac.id (A. B. Aritonang), rezaaudina002@gmail.com (R. A. Putri), vivi009@brin.go.id (V. Sisca), mjihad1991@gmail.com (M. J. Madiabu), khoi013@brin.go.id (K. Khoiriah).

https://doi.org/10.21123/2411-7986.4960

irradiation, sol-gel, hydrothermal methods, co-precipitation, flame spray pyrolysis, wet chemical methods, and spin coating.[7–9] However, these traditional procedures necessitate the use of harmful chemicals, as well as high pressure and temperatures. Conventional techniques not only produce dangerous byproducts, but they also have inferior stability due to their great inclination to agglomerate.[10,11]

The synthesis of TiO_2 NPs using green approaches, i.e. employing phytochemical extracts, has gained popularity because these methods are both cost-effective and environmentally beneficial due to the use of safe ingredients and the release of non-hazardous end products. Secondary metabolites found in phytochemical extracts, including flavonoids, terpenoids, sugars, polyphenols, alkaloids, peptides, and terpenoids, are hypothesized to be responsible for metal ion conversion to NPs. According to the traditional concept of green chemistry, phytoconstituents in plants should perform at least one of the following functions: Metal salt reduction, Ti^{4+} precursor hydrolysis, and intermediate solubilization and polymerization.[1] Synthesis with phytochemical extracts can yield stable and dispersible NPs with variable size in an environmentally responsible and cost-effective manner. The metabolites operate as reducing and capping agents, regulating the pH of the medium and, as a result, the phase morphology of the NPs.[10]

The peels of Petai (*Parkia speciosa*) are usually disposed of as solid waste, polluting the environment. They contain secondary metabolites such as phenols, terpenoids and flavonoids, which have the potential to act as reducing and capping agents in the synthesis of magnetite, tin oxide, and biosilver nanoparticles[12–14] and there has been no report of using aqueous petai peel extract to synthesize TiO_2 nanoparticles.

Acid Yellow 25 (AY) is a dye that is commonly used in the textile industry to dye natural fibers such as cotton, wool, and silk, as well as synthetic fibers such as nylon, rayon, polyester, and acrylicin weakly acidic solutions at pH 2 to 6, where the name “acid” comes from the dyeing process. Acid dyes are predominantly mono-azo compounds, although they may also comprise diazo, nitro, 1-amino anthraquinone, triphenylmethane, and other groups of chemicals. Their structure contains sulfonic groups, which causes them to be anionic.[15]

The purpose of this research is to prepare nanoparticles TiO_2 via the green method mediated by aqueous *Parkia speciosa* peel extract and to evaluate the photocatalytic activity of the obtained nanoparticles TiO_2 on the reduction of AY dyes at various catalyst doses, initial AY concentrations, and solution pH.

Materials and methods

Preparation of petai peel extract

The fresh, fully ripened peels of petai (PP) were collected from the traditional market of South Tangerang, Indonesia. Before cutting, the peels were washed with water to remove all impurities. The clean PP were dried, ground and sieved using a 100 mesh sieve. About two grams of PP powder was macerated in 100 ml of Aquadest for 24 hours and filtered to obtain the extract as a reducing and capping agent. The PP extract was stored in the refrigerator for further use.

Synthesis of nanoparticle TiO_2 NPs

All materials used in this research are shown in Table 1. The synthesis procedure originates from Saka’s research, whereby the pH solution, synthesis and calcination temperature was modified.[16] About 100 mL of titanium isopropoxide (TTIP, 0.2 M) was added dropwise with 20 mL of PP extract under constant stirring for 5 hours at room temperature, as shown in Fig. 1. The gel as a product was centrifuged and washed three times with Aquadest. A brown precipitate was dried in an oven at 80°C and calcined at 490°C for 2 hours to obtain white PP-TiO_2 NPs powder.[9]

Characterization of TiO_2 NPs

The prepared PP-TiO_2 NPs were analyzed by optical, physical, and surface studies. The structural

Table 1. Materials used for the research.

No	Chemicals	Purcahsed from
1	Titanium Tetra isopropoxide (TTIP, purity > 95%)	Sigma Aldrich
2	Acid Yellow 25	Merck
3	Commercial TiO_2	low grade
4	Iso-propanol	Merck
5	Sodium hydroxide (NaOH)	Merck
6	Hydrochloric acid (HCl)	Merck
7	Petai peels (PP)	Traditional market in Serpong, Indonesia.

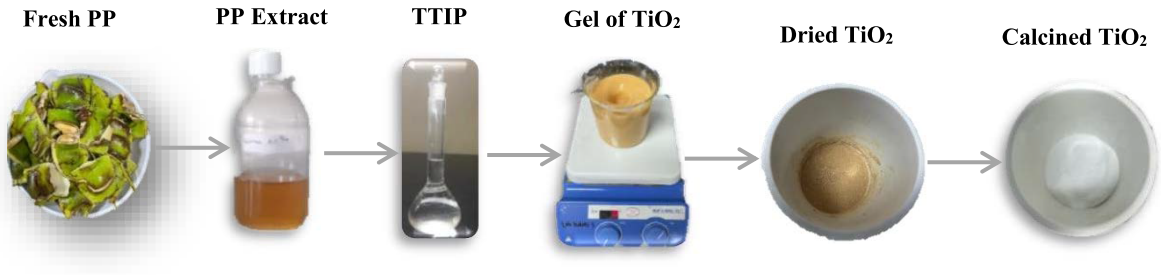

Fig. 1. Synthesis procedure of P-TiO2-NPs mediated by PP extract.

properties of the PP-TiO_2 NPs were determined using an X-ray diffractometer (XRD PANalytical EMPYREAN with Cu- Kα radiation, k= 1.54 Å). The XRD data were used to calculate the crystallite size using the Scherrer formula. The optical properties were observed using a Shimadzu 2700 UV-DRS spectrophotometer, and the results were utilized to calculate the band gap of PP-TiO_2 NPs using the Kubelka-Munk equations in Eq. (1) and Eq. (2). $R_\infty = \frac{R\ Sample}{R\ Standard}$ represents the reflectance of an infinitely thick specimen. K and S are the absorption and scattering coefficients, respectively. Where h, ν, Eg, B, is the Planck constant, the photon's, the band gap energy, and a constant, respectively. The γ factor depends on the nature of the electron transition and is equal to $^1/_2$ or 2 for the direct and indirect transition band gaps, respectively.

$$F(R_\infty) = \frac{K}{S} = \frac{(1-R_\infty)^2}{2R_\infty} \quad (1)$$

$$\left(F(R_\infty).\ h\nu\right)^{1/\gamma} = B\left(h\nu - E_g\right) \quad (2)$$

The morphology, particle size, and surface structure were analyzed using a field emission scanning electron microscope (FE-SEM, Carl ZEISS, Germany) in conjunction with EDS (JEOL model 6390). Fourier transform infrared spectroscopy (FTIR, Bruker Tensor II), Raman spectrometer (HORIBA), zeta analyzer (HORIBA SZ-100) and nanoparticle size analyzer (Microtrac MRB) were used for the binding structures of the phytochemicals in the PP extract, zeta potential and particle sizes. The pH_{zpc} of prepared TiO_2 was determined using the adsorption method described by Jayan and and Metta.[17] About 0.1g of TiO_2 nanoparticles were added to 30 ml of a 0.01 M NaCl solution. The initial pH of the solution was adjusted from 2 to 10 in each bottle by adding 0.1M HCl or 0.1M NaOH. The final pH of the solution was measured after shaking at room temperature for 24 hours and removing the TiO_2 nanoparticles. The intersection between the initial pH (pH_i) and the difference value (ΔpH) represented the zero-point charge of the TiO_2 nanoparticles.[17]

Reduction of dyes experiment

The activity of PP-TiO_2 NPs was used to reduce AY dyes. The PP-TiO_2 NPs catalyst dyes were added to the dye solution (15 mg L^{-1}) with steady stirring and allowed to reach equilibrium before being exposed to 2×20 W UV light. The dye solution was taken out at 30-minute intervals for up to 120 minutes. The catalyst was removed by centrifugation of the withdrawn 4 mL solution at 10,000 rpm for 10 minutes. UV-visible spectroscopy at a wavelength of 395 nm was used to measure the reduction in dye concentration. Eq. (3) was used to compute removal percentage, with AY_i and AY_f representing the dyes' initial and final concentrations, respectively. The investigated parameters of reduction process were the catalyst dose, the initial concentration of the dyes and the initial pH of the solution. Direct photolysis and adsorption of PP-TiO_2 NPs were also performed as controls.

$$\text{Removal}\ (\%) = \frac{\text{AYi} - \text{AYf}}{\text{AYi}} \text{ x } 100 \quad (3)$$

Results and discussion

FTIR and raman spectra

FT-IR spectroscopy was used to identify the probable biomolecules based on chemical groups contained in the PP extract responsible for the capping or reduction of the precursor, which plays a key role in the synthesis of TiO_2 nanoparticles. The FT-IR spectrum of PP extract and prepared TiO_2 is shown in Fig. 2a. The peaks of PP extract spectra appeared at wavenumbers 3262, 1634, 509 cm^{-1}, which corresponded to hydroxyl groups (O-H), carbonyl groups (C=O), and aromatic groups (C=C), respectively.[18]

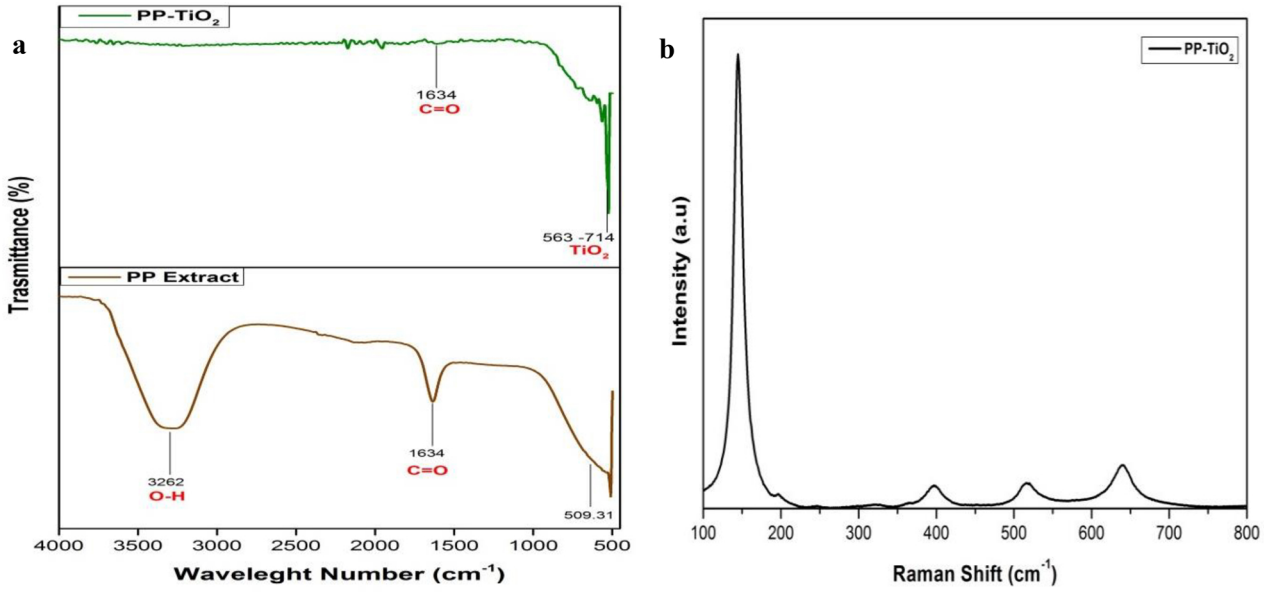

Fig. 2. (a) FTIR and (b) Raman spectra of PP-TiO_2 mediated by PP extract.

According to the Huey-Jiun Ko et al research the main compounds in the aqueous PP extract are polyphenol and flavonoid such as gallic acid > ellagic acid > quercetin > epicatechin.[19] which plays an important role as capping and reducing agents in the formation of nanoparticle TiO_2. Gallic acid contains hydroxyl and carboxyl groups coordinating with titania's surface hydroxyl groups2.[20] Moreover, the C=O groups at 1634 cm^{-1} and Ti-O-Ti vibration at spectra below 1000 cm^{-1} were detected in the spectral band of PP-TiO_2 nanoparticles which could be due to the improved precision of the prepared nanoparticles in anatase crystal form after calcination at 490°C. The data suggest that polyphenol and flavonoid groups played an essential role as capping, stabilizing and reducing agents in the synthesis of the nanoparticles. Ansari et al. found the same FTIR trend on their reseacrch of synthesis TiO_2 nanoparticles using *Acorus calamus* leaf extract.[21]

Fig. 2b reveals five active Raman modes: an intense peak at 144.5 cm^{-1}, followed by low intensity peaks at 397.3, 516.2, and 639.6 cm^{-1}, which correspond to Eg(1), B1g, A1g, and Eg(3), respectively. The intense peak at 144.5 corresponds primarily to the symmetric stretching vibration of TiO_2, whereas the weak intensity peaks at 397.3 clearly show the symmetric bending vibration of O-Ti-O, and the peak at 516.2 corresponds to the antisymmetric bending vibration of O-Ti-O. These unique vibrational frequencies and intensity ratios confirmed the high-purity anatase phase, tetragonal TiO_2 nanostructure free of impurities. The raman spectra of the prepared TiO_2 NPs is well matched with the spectra of TiO_2 NPs prepared mediated by *Aspergillus eucalypticola SLF1*[22] and coffee husk.[23]

Difractogram of PP-TiO_2 NP

Fig. 3 shows the X-ray diffraction pattern of the synthesised PP-TiO_2 NPs. It shows intense and broad peaks, indicating that the particles are present as very small crystallites. The peak positions and their intensities are in good agreement with the standard (ICDD NO: 98-004-4882) and commercial powder diffraction patterns of anatase TiO_2. It showed a main peak

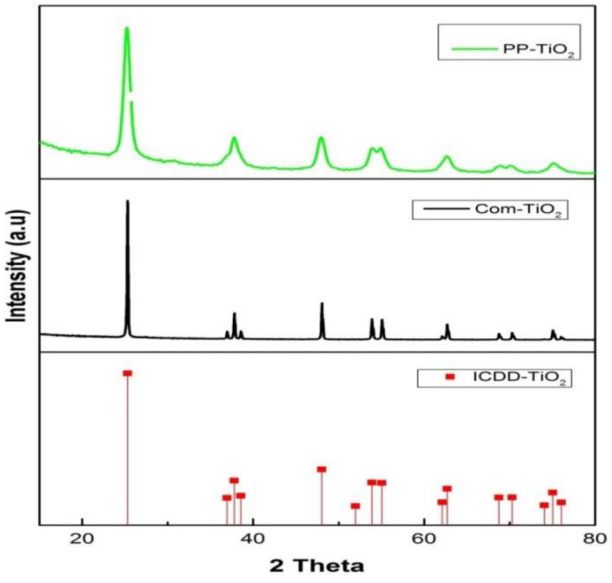

Fig. 3. Difractoghram of PP-TiO_2 mediated by PP extract.

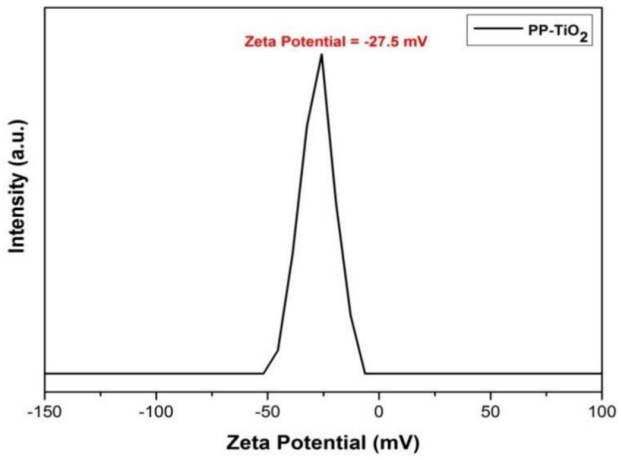

Fig. 4. Zeta potential of PP-TiO_2 mediated PP extract.

at 25.28° corresponding to the (101) plane and other peak positions at 37.79° (004), 48.98° (200), 53.93° (105), 54.93° (211), 62.70° (204). These values correspond to the tetragonal structure and the anatase phase of the TiO_2 NPs. The average crystallite size calculated with the Scherer equation is 8.232 nm. This interfering peak shows that the sample contains a pure anatase phase. The small crystallites and the anatase phase are useful for photocatalysis of organic pollutants.[24] The phase-pure TiO_2 nanostructure has explored the superior activities in water treatment and microbial resistant areas. The results of XRD analysis confirmed that the synthesised TiO_2 NPs were polycrystalline.[25]

Zeta potential of PP-TiO_2 NPs

The zeta potential of prepared PP-TiO_2 was investigated using dynamic light scattering instrument (DLS). The determined zeta potential was –27.5 mV, indicating quite stable particles, a good colloidal nature and a high stability of TiO_2 in aqueous solutions Fig. 4. The suspended colloidal system is stable when the zeta potential is less than −25mV or greater than +25 mV.[26] The negative sign of the zeta potential indicates that the negatively charged phytochemicals cause repulsion and prevent agglomeration of the TiO_2 NPs. This condition was crucial for their improvement and long-lasting stability.[27]

Band gap of PP-TiO_2 NPs

The band gap value of prepared TiO_2 using PP extract was determined by an indirect method using the Kubelka-Munk Eq. (1)–Eq. (2). The calculated band gap for PP- TiO_2 NPs was 3.26 eV, which is smaller than the band gap value of commercial TiO_2 (Egap = 3.31 eV), as shown in Fig. 5. The presence of PP extract in the synthesis process leads to a slight decrease in the TiO_2 band gap. The same phenomenon was also observed by Alobaidi et al. in biosynthesis of titanium dioxide nanoparticles using *Zizyphus Spina-Christi* leaves.[28]

Field emission electron microscopy (FE-SEM)

SEM images were also collected to establish the average grain size and shape of the NPs. The FE-SEM image confirms that the prepared PP-TiO_2 NPs are spherical Fig. 6. The size of PP-TiO_2 ranged from 16 to 22 nm, which was less than that of commercial TiO_2 (about 1450 nm) and to the produced TiO_2 from other peels extract as depicted in Table 2.

The size distribution of the synthesised TiO_2 NPs was also measured using DLS analyzer. The data

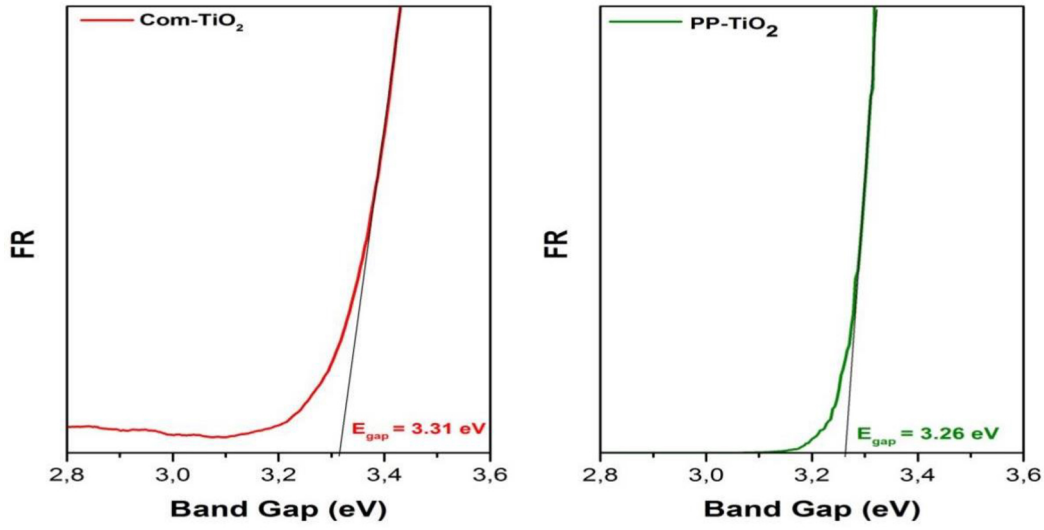

Fig. 5. Band gap of PP-TiO_2 mediated PP extract.

Table 2. The PP-TiO_2 NPs mediated by PP extract compared to the other aqoeous peel extract.

Titanium precursor	Peel extract prepared from (Aqeous)	Phytochemical resources	Crystalline Phase	Particle size (nm)	References
TTIP	Onion & garlic	*Allium cepa L. & Allium sativum*	Anatase	10–22	[29]
TTIP	Mangosteen pericarp	*Garcinia mangostana*	Anatase & Rutile	147	[30]
TTIP	Tangerine	*Citrus reticulata*	Anatase & Rutile	50–150	[31]
TiO_2 bulk powder	Banana	*Musa paradaisica*	-	88	[32]
TTIP	Pomegranate	*Punicagranatum*	Anatase	93	[33]
$Ti(NO_3)_4$	rambutan	*Nephelium Lappaceum L*	Anatase	70–90	[34]
TiO_2 bulk powder	Lemon	*Citrus limon*	Anatase	80–140	[35]
TTIP	Potato	*Solanum tuberosum*	Anatase	27	[36]
$TiCl_3$	Mango-peel	*Mangifera indica*	Anatase	16.9	[37]
TTIP	Orange	-	Anatase	75–85	[38]
TTIP	Beet	*Beta vulgaris*	Anatase	9.09	[39]
TiO_2 bulk powder	Plum,	*P. domestica L*	Anatase	47–63	[40]
	Kiwi	*P. Persia L.*	Anatase	54–85	
	Peach	*A. deliciosa*	Anatase	200	
TTIP	Petai	*Parkia speciosa*	Anatase	16.6	This study
$TiCl_4$	Orange	*Citrussinesis*	Anatase	17–21	[41]

showed the typical size of TiO_2 of ~48.60 nm indicating the nanopraticles types. Theese results revealed that the PP-TiO_2 was was composed of nano-sized particles of the same format. The high-quality dispersion of PP-TiO_2 can be attributed to the remaining phytoconstituents of the PP extract, such as flavonoids, polyphenols, and alkaloids, which facilitated the stabilization of the resulting TiO_2 NPs and thus improved the NPs' dispersion by preventing agglomeration.[42] Nano-sized particles provide a high surface area in the configuration of the TiO_2 enclosure, which could help in the inhibition of bacteria and the treatment of wastewater pollution.[28]

Application of PP-TiO_2 as photocatalyst in AY dye reduction

The photocatalytic activity of the prepared TiO_2-NPs was investigated for the degradation of Acid Yelow 25 (AY) dyes. The reduction of dyes concentration during the photocatalysis was converted to be removal percentage using Eq. (3). The photodegradation studies were validated by the standard deviation (maximum 4.8%) and the result were shown in Fig. 7. The catalyst dose is the most important parameter that determines the rate of the reduction process of organic pollutants. The amount of PP-TiO_2 NPs added to the AY dye solution was in the range of 0.1–0.3 g. The AY dyes were removed at 59. 73%, 65.935% and, 69.65% with the addition of 0.1 g, 0.2 g and 0.3 g of catalyst, respectively. This result was explained by the increase in catalyst dose, which provides a hinger active site and more photons adsorbed in the surface of PP-TiO_2 NPs for the oxidative species formation in the photocatalytic removal of AY dyes.[43] Direct photolysis and adsorption were also performed as controls in this study. Fig. 7a shows that the two methods were not effective in removing AY dyes, with an removal percentage of 6.675% for

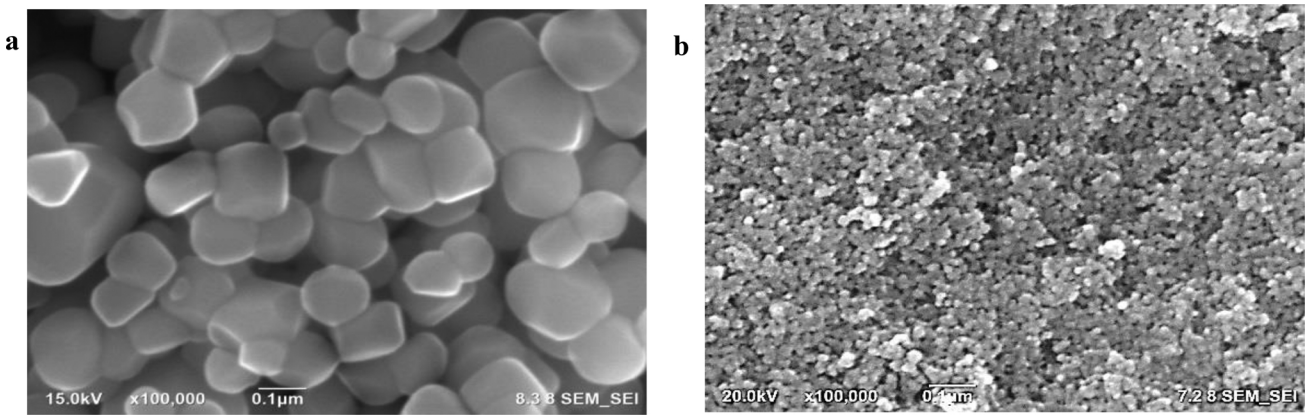

Fig. 6. FE-SEM image of (a) commercial TiO_2 and (b) PP-TiO_2 mediated PP extract.

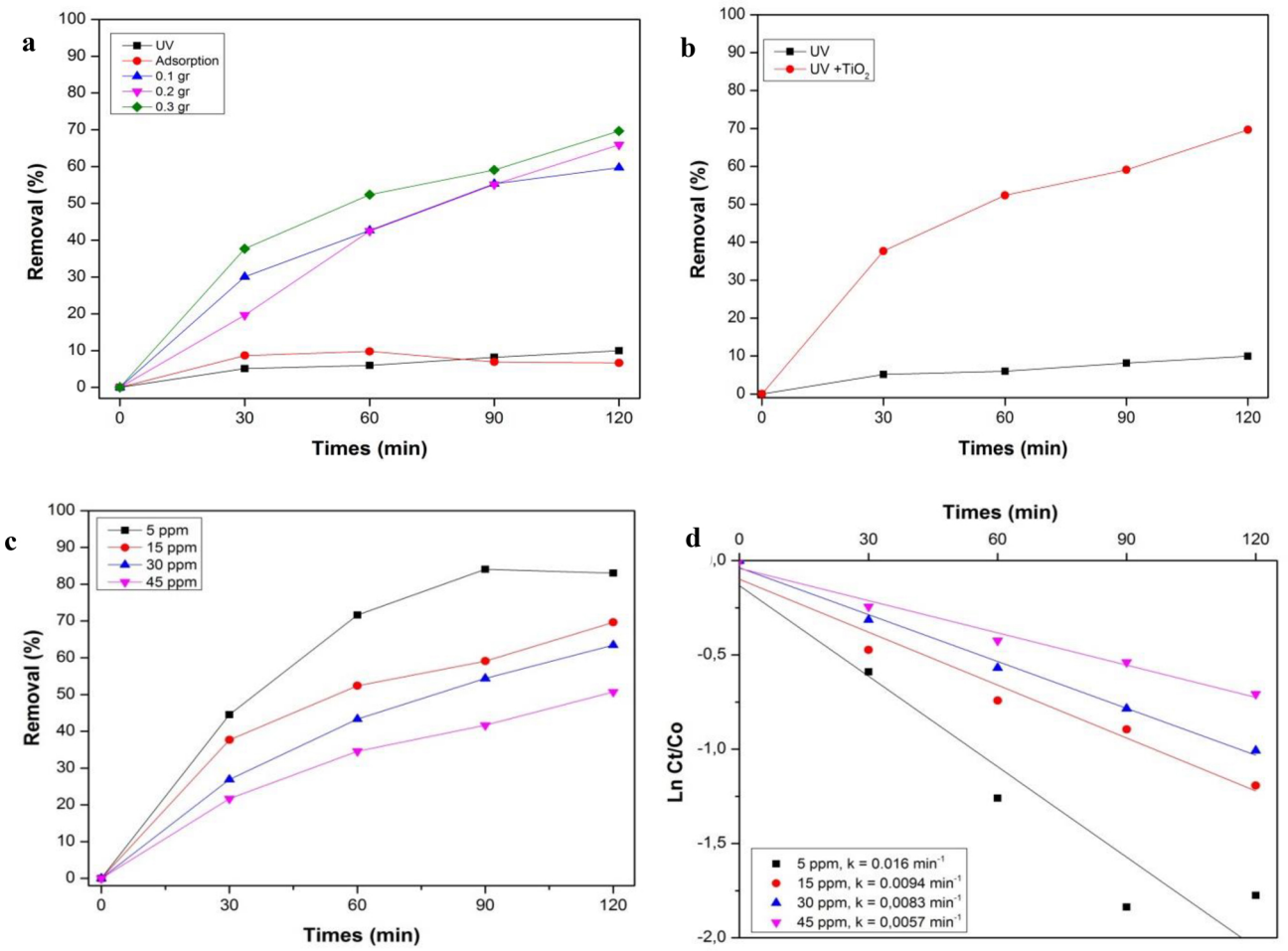

Fig. 7. The effect of (a) catalyst dose, (b) the presence of PP-TiO_2 NPs catalyst (c) initial concentration dyes, and (d) kinetic rate, on AY reduction.

adsorption and 9.975% for direct UV- photolysis. In the presence of PP-TiO_2 NPs, the removal percentage increased significantly 5.98-fold compared to direct photolysis as shown in Fig. 7b. The electron of PP-TiO_2 NPs was excited from the valence band to the conduction band in the presence of UV light energy. This process generates a hole (h^+), an electron (e^-) and a hydroxyl radical (^-OH), which oxidizes the AY dyes to simpler compounds such as CO_2 and H_2O as shown in Fig. 8c.[44,45]

Another important variable for the reduction percentage was the concentration of organic pollutants. As can be seen in Fig. 7c, the removal percentage decreased with increasing AY dye concentration. At an initial concentration of 5 ppm, about 83.05% of the AY dye was reduced. At 15 ppm, 30 ppm and 45 ppm, it was only 69.65%, 63.465% and 50.715% of the initial concentration, respectively. The possible reason for the decreasing removal percentage at a higher initial concentration of the AY dye is that more reactant molecules are adsorbed on the catalyst surface and block the active sites of the PP-TiO_2 NPs catalyst. Another reason is that more intermediates are formed, which are adsorbed and block and deactivate the active sites of the catalyst. The result was a good correlation with the kinetic rate data in Fig. 7d. The kinetic rate of AY dye reduction was 2.8 times faster at an initial concentration of 5 ppm than at the other three initial concentrations.

As the initial concentration of the dye increases, dye molecules are adsorbed on the catalyst's surface, and the dye molecules absorb a large quantity of light rather than the TiO_2 particles. As a result, the amount of light that can penetrate the catalyst's surface diminishes. The formation of hydroxyl radicals has decreased as dyes have filled the active sites. Because there is no direct contact between the semiconductor and the photocatalyst, the adsorbed dye prevents the interaction of adsorbed molecules with photo-induced positive holes or hydroxyl radicals. A high dye concentration also protects UV light. This lowers the length of the photon's travel through the

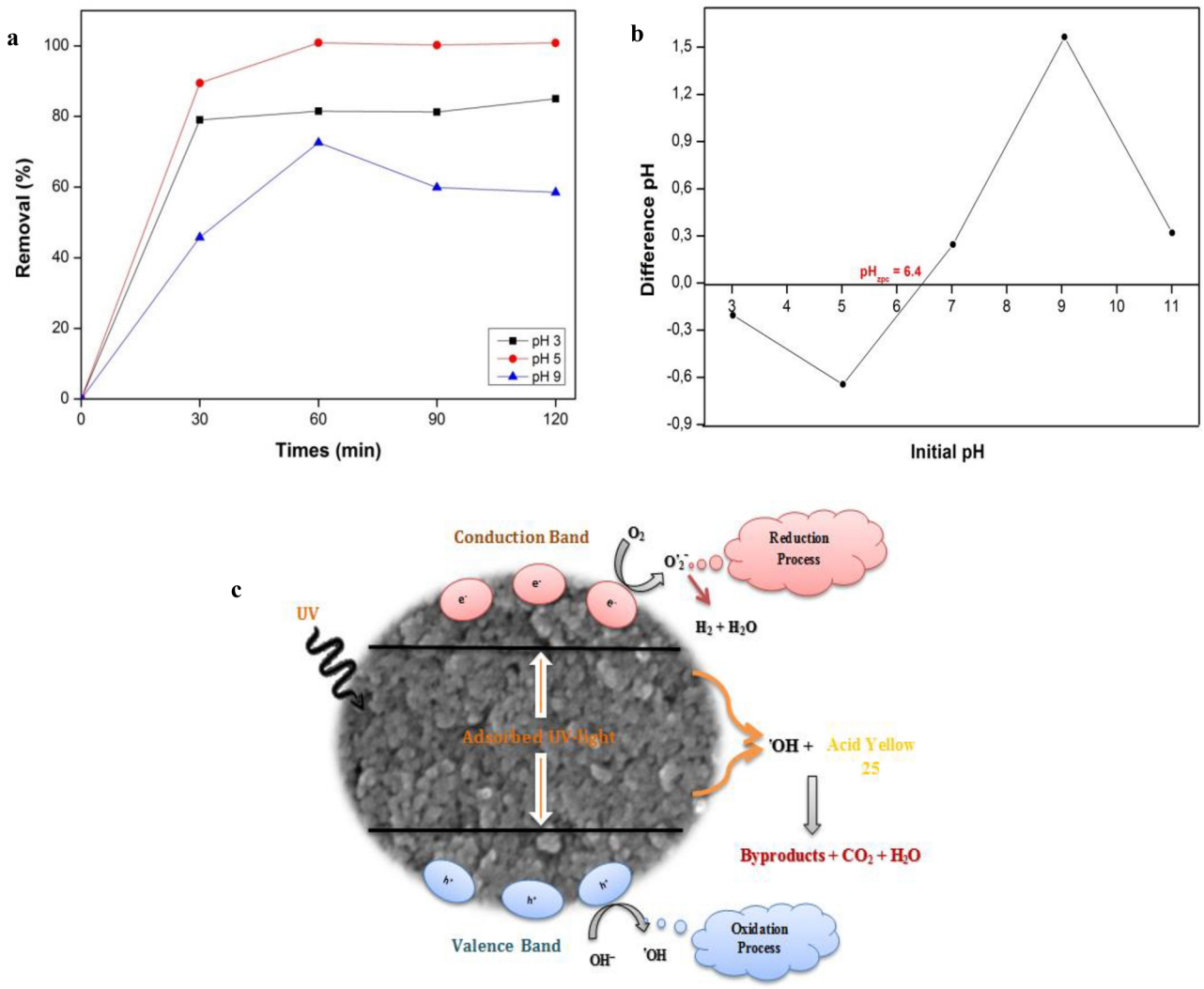

9

Fig. 8. (a) The effect of initial pH on AY reduction using PP-TiO_2 NPs, (b) Zero point charge of PP-TiO_2 NPs (c) reduction process of AY dyes using prepared PP-TiO_2 NPs.

solution. Again, as the initial concentration of the dye increases, so does the amount of catalyst surface needed for degradation. Because the illumination time and catalyst amount are constant, the OH radical (primary oxidant) generated on TiO_2's surface is also constant. As a result, the relative quantity of free radicals attacking the dye molecules falls with increasing dye concentration. [46]

The effect of the initial pH value of the dye solution was also investigated in this experiment in order to achieve an optimal reaction condition. The pH of the dye solution was adjusted to 3, 7 and 9 by using HCl or NaOH. The AY dye was reduced by 85%, 100% and 83% at pH 3, 5 and 9 respectively. The optimum pH was reached at pH 5, as shown in Fig. 8a. This result could be explained by the pH zero charge of TiO_2 about 6.4 as depicted in Fig. 8b. [43] AY as an anionic dye is optimally adsorbed on the surface of PP-TiO_2 NPs at pH 5, since under this condition the charge of PP-TiO_2 NPs is positive. As a result, the reduction process increases significantly. In contrast, at higher pH values, there was a repulsion between the negatively charged catalyst and the anionic AY dyes, which led to a decrease in the reduction process. [47] Tang et al also found that photocatalysis of AY dye with TiO_2 as a catalyst works better at acidic pH than at basic pH. [48]

Conclusion

The PP-TiO_2-NPs was successfully prepared mediated by PP extract as a reducing and capping agents. The physicochemical properties of the prepared

PP-TiO_2-NPs were investigated by XRD, FESEM, FTIR, UV-DRS, Raman and zeta analyzer. According to the characterization results, the obtained TiO_2 were pure crystalline, in the anatase phase, stable particles and spherical with a size of 16 to 22 nm. FTIR data showed that the PP compounds such as polypenol and flavonoids acted as sustainable reducing and capping agents. The prepared TiO_2 completely reduced AY dye at pH 5 for 120 minutes. The photoreduction followed the first-order model kinetics with a reaction rate constant of 0.016 min^{-1}. The present study revealed that the prepared TiO_2-NPs exhibited enhanced photocatalytic activity in AY dye reduction. These outstanding results will encourage researchers to explore the possibilities offered by nature and develop innovative and safer methods for the synthesis of metal oxide nanomaterials.

Acknowledgment

This work was supported by Research Organization of Nanotechnology and Material, National Research and Innovation Agency (BRIN), Indonesia.

Authors' declaration

- Conflicts of Interest: None.
- We hereby confirm that all the Figures and Tables in the manuscript are ours. Furthermore, any Figures and images, that are not ours, have been included with the necessary permission for republication, which is attached to the manuscript.
- No animal studies are present in the manuscript.
- No human studies are present in the manuscript.
- Ethical Clearance: The project was approved by the local ethical committee at National Research and Innovation Agency (BRIN), Indonesia.

Authors' contribution statement

A. B. A: funding, acquisition, interpretation, R. A. P: methodology, supervision, V. S: acquisition of data, revision and proofreading, M. J. M.: analysis, acquisition of data, K. K: conception, design, acquisition of data, drafting the MS, revision and proofreading. All authors read and approved the fnal manuscript.

References

1. Abdelaty M, Ghazal H. Nanotechnology and application of nano titanium dioxide, nano zinc oxide, and nano copper oxide on textile for high performance. Egypt J Chem. 2023;66(3):309–322. https://doi.org/10.21608/EJCHEM.2022.132895.5868.
2. Rajaram P, Jeice AR, Jayakumar K. Review of green synthesized TiO_2 nanoparticles for diverse applications. Surf Interfaces. 2023;39:(102912). https://doi.org/10.1016/j.surfin.2023.102912.
3. Mohsen Mhadhbi, Abderazzak H, Avar B. Synthesis and properties of titanium dioxide nanoparticles. IntechOpen. 2023. http://dx.doi.org/10.5772/intechopen.111577.
4. Hameed HG, Abdulrahman NA. Synthesis of TiO_2 nanoparticles by hydrothermal method and characterization of their antibacterial activity: Investigation of the impact of magnetism on the photocatalytic properties of the nanoparticles. Phys Chem Res. 2023;11(4):771–782. https://doi.org/10.22036/pcr.2022.351688.2137.
5. Munonde TS, Raphulu MC. Review article review on titanium dioxide nanostructured electrode materials for high-performance lithium batteries. J Energy Storage. 2024;78:(110064). https://doi.org/10.1016/j.est.2023.110064.
6. Lakra R, Kumar R, kumar S, Thatoi D, Soam A. Synthesis of TiO_2 nanoparticles as electrodes for supercapacitor. Mater Today. 2023;74:863–866. https://doi.org/10.1016/j.matpr.2022.11.271.
7. Permana MD, Noviyanti AR, Lestari PR, Kumada N, Eddy DR, Rahayu I. Synthesis and photocatalytic activity of TiO_2 on phenol degradation. Kuwait J Sci. 2022;49(4):1–13. https://doi.org/10.48129/kjs.13509.
8. Fayyadh AA, Essa AF, Batros SS, Shallal ZS. Studying the crystal structure, topography, and anti-bacterial of a novel titania (TiO_2 NPs) prepared by a sol-gel manner. Baghdad Sci J. 2019;16(4):910–918. http://dx.doi.org/10.21123/bsj.2019.16.4.0910.
9. Verma V, Al-Dossari M, Singh J, Rawat M, Kordy MGM, Shaban M. A review on green synthesis of TiO_2 NPs: Photocatalysis and antimicrobial applications. Polymer. 2022;14(7):1–19. https://doi.org/10.3390/polym14071444.
10. Roy J. Review the synthesis and applications of TiO_2 nanoparticles derived from phytochemical sources. J Ind Eng Chem. 2022;106:1–19. https://doi.org/10.1016/j.jiec.2021.10.024.
11. Ying S, Guan Z, Ofoegbu PC, Clubb P, Rico C, Feng Hea JH. Green synthesis of nanoparticles: Current developments and limitations. Environ Technol Innov. 2022;26(102336):1–20. https://doi.org/10.1016/j.eti.2022.102336.
12. Azhar FH, Harun Z, Yusof KN, Alias SS, Hashim N, Sazali ES. A study of different concentrations of bio-silver nanoparticles in polysulfone mixed matrix membranes in water separation performance. J Water Process Eng. 2020;38:101575. https://doi.org/10.1016/j.jwpe.2020.101575.
13. Begum S, Ahmaruzzaman M. Bio-inspired green synthesis of reclaimable ZnO nanoclusters using *Parkia speciosa Hassk* pods and its potential photocatalytic removal of waterborne pollutant and antioxidant activities. J Mater Sci.: Mater Electron. 2021;32:12042–12058. https://doi.org/10.1007/s10854-021-05834-5
14. Rahmayanti M, Syakina AN, Sulistyaningsih T, Hastuti B. Synthesis of magnetite using petai (*Parkia speciosa*) peel extract with ultrasonic waves as reusable catalysts for biodiesel production from waste frying oil. J Kim Sains Apl. 2023;26(4):125–132. https://doi.org/10.14710/jksa.26.4.125-132.
15. Wei C-C, Pathiraja IK, Fabry E, Schafer K, Schimp N, Hu T-P *et al.* Removal of acid yellow 25 from aqueous solution by chitin prepared from waste snow crab legs. J Encapsulation Adsorpt Sci. 2018;8:139–155. https://doi.org/10.4236/jeas.2018.83007.

16. Saka A, Shifera Y, Jule LT, Badassa B, Nagaprasad N, Shanmugam R *et al.* Biosynthesis of TiO_2 nanoparticles by Caricaceae (Papaya) shell extracts for antifungal application. Sci Rep. 2022;12(1):1–10. https://doi.org/10.1038/s41598-022-19440-w.
17. Jayan N, Metta LDB. Process optimization by response surface methodology-central composite design for the adsorption of lead by green synthesized TiO_2 using Phyllanthus acidus extract. Biomass Convers Biorefin. 2022:1–21. https://doi.org/10.1007/s13399-022-02534-w.
18. Ahmad W, Jaiswal KK, Soni S. Green synthesis of titanium dioxide (TiO_2) nanoparticles by using Mentha arvensis leaves extract and its antimicrobial properties. Inorg Nano-Met Chem. 2020;50(10):1032–1038. https://doi.org/10.1080/24701556.2020.1732419.
19. Azemi AK, Nordin ML, Hambali KA, Noralidin NA, Mokhtar SS, Rasool AHG. Phytochemical contents and pharmacological potential of parkia speciosa hassk. for diabetic vasculopathy: A review. Antioxidants. 2022;11(431):1–14. https://doi.org/10.3390/antiox11020431.
20. Bakun P, Czarczynska-Goslinska B, Mlynarczyk DT, Musielak M, Mylkie K, Dlugaszewska J *et al.* Gallic acid-functionalized, TiO_2-based nanomaterial-preparation, physicochemical and biological properties. Materials. 2022;15(12):1–19. https://doi.org/10.3390/ma15124177.
21. Ansari A, Siddiqui VU, Rehman WU, Akram MK, Siddiqi WA, Alosaimi AM *et al.* Green synthesis of TiO_2 nanoparticles using Acorus calamus leaf extract and evaluating its photocatalytic and in vitro antimicrobial activity. Catalysts. 2022;12(2):1–18. https://doi.org/10.3390/catal12020181.
22. Survase AA, Kanase SS. Green synthesis of TiO_2 nanospheres from isolated Aspergillus eucalypticola SLF1 and its multifunctionality in nanobioremediation of C. I. Reactive Bluec 194 with antimicrobial and antioxidant activity. Ceram Int. 2023;49:14964–14980. https://doi.org/10.1016/j.ceramint.2023.01.079.
23. Al Qarni F, Alomair NA, Mohamed HH. Environment-friendly nanoporous titanium dioxide with enhanced photocatalytic activity. Catalysts. 2019;9(10):1–13. https://doi.org/10.3390/catal9100799.
24. Vishali D, Manikandan B, John R, Murali KR. Degradation of methylene blue dye by TiO_2 nanoparticles biologically synthesized using leaf extract of citrus aurantifolia. Trans Electr Electron Mater. 2021;22(5):622–629. https://doi.org/10.1007/s42341-020-00270-4.
25. Rathi VH, Jeice AR. Green fabrication of titanium dioxide nanoparticles and their applications in photocatalytic dye degradation and microbial activities. Chem Phys Impact. 2023;6(100197):1–13. https://doi.org/10.1016/j.chphi.2023.100197.
26. Rajeswari VD, Eed EM, Elfasakhany A, Badruddin IA, Kamangar S, Brindhadevi K. Green synthesis of titanium dioxide nanoparticles using Laurus nobilis (bay leaf): antioxidant and antimicrobial activities. Appl Nanosci. 2023;13(2):1477–1484. https://doi.org/10.1007/s13204-021-02065-2.
27. Ur Rehman K, Zaman U, Tahir K, Khan D, Khattak NS, Khan SU *et al.* A Coronopus didymus based eco-benign synthesis of Titanium dioxide nanoparticles (TiO_2 NPs) with enhanced photocatalytic and biomedical applications. Inorg Chem Commun. 2022;137(109179):1–10. https://doi.org/10.1016/j.inoche.2021.109179.
28. Alobaidi T, Alwared A. Biosynthetic of titanium dioxide nanoparticles using *Zizyphus Spina*-Christi leaves extract. J Ecol Eng. 2022;23(1):315–324. https://doi.org/10.12911/22998993/143971.
29. Ali H, Dixit S, Almutairi BO, Yadav N. Synthesis and characterization of eco-friendly TiO_2 nanoparticle from combine extract of onion and garlic peel. J King Saud Univ Sci. 2023;35(8):1–7. https://doi.org/10.1016/j.jksus.2023.102918.
30. Ahn EY, Shin SW, Kim K, Park Y. Facile green synthesis of titanium dioxide nanoparticles by upcycling mangosteen (Garcinia mangostana) pericarp extract. Nanoscale Res Lett. 2022;17(1):1–12. https://doi.org/10.1186/s11671-022-03678-4.
31. Rueda D, Arias V, Zhang Y, Cabot A, Agudelo AC, Cadavid D. Low-cost tangerine peel waste mediated production of titanium dioxide nanocrystals: Synthesis and characterization. Environ Nanotechnol Monit Manag. 2020;13(100285):1–7. https://doi.org/10.1016/j.enmm.2020.100285.
32. Hameed RS, Fayyad RJ, Nuaman RS, Hamdan NT, Maliki SAJ. Synthesis and characterization of a novel titanium nanoparticals using banana peel extract and investigate its antibacterial and insecticidal activity. J Pure Appl Microbiol. 2019;13(4):2241–2249. https://doi.org/10.22207/jpam.13.4.38.
33. Muna Abu-Dalo, Azza Jaradat, Borhan A Albiss, Al-Rawashdeh NAF. Green synthesis of TiO_2 NPs/pristine pomegranate peel extract nanocomposite and its antimicrobial activity for water disinfection. J Environ Chem Eng. 2019;7(5):1–13. https://doi.org/10.1016/j.jece.2019.103370.
34. Isacfranklin M, Yuvakkumar R, Ravi G, Kumar P, Saravanakumar B, Velauthapillai D *et al.* Biomedical application of single anatase phase TiO_2 nanoparticles with addition of Rambutan (Nephelium lappaceum L.) fruit peel extract. Appl Nanosci. 2020;11(2):699–708. https://doi.org/10.1007/s13204-020-01599-1.
35. Nabi G, Ain Q-U, Tahir MB, Nadeem Riaz K, Iqbal T, Rafique M *et al.* Green synthesis of TiO_2 nanoparticles using lemon peel extract: their optical and photocatalytic properties. J Environ Anal Chem. 2020;102(2):434–442. https://doi.org/10.1080/03067319.2020.1722816.
36. Girigoswami A, Deepika B, Pandurangan AK, Girigoswami K. Preparation of titanium dioxide nanoparticles from solanum tuberosum peel extract and its applications. Artif Cells Nanomed Biotechnol. 2024;52(1):59–68. https://doi.org/10.1080/21691401.2023.2301068.
37. Isnaeni IN, Indriyati, Dedi, Sumiarsa D, Primadona I. Green synthesis of different TiO_2 nanoparticle phases using mango-peel extract. Mater Lett. 2021;294(129792):1-5. https://doi.org/10.1016/j.matlet.2021.129792.
38. Oleiwi HF, Rahma AJ, Salih SI, Beddai AA. Comparative study of sol-gel and green synthesis technique using orange peel extract to prepare TiO_2 nanoparticles. Baghdad Sci J. 2023;21(15):1702–1711. https://doi.org/10.21123/bsj.2023.8089.
39. Jayapriya M, Arulmozhi M. Beta vulgaris peel extract mediated synthesis of Ag/TiO_2 nanocomposite: Characterization, evaluation of antibacterial and catalytic degradation of textile dyes-an electron relay effect. Inorg Chem Commun. 2021;128(108529). https://doi.org/10.1016/j.inoche.2021.108529.
40. Ajmal N, Saraswat K, Bakht MA, Riadi Y, Ahsan MJ, Noushad M. Cost-effective and eco-friendly synthesis of titanium dioxide (TiO_2) nanoparticles using fruit's peel agro-waste extracts: characterization,in vitroantibacterial, antioxidant activities. Green Chem Lett Rev. 2019;12(3):244–254. https://doi.org/10.1080/17518253.2019.1629641.

41. Fall A, Ngom I, Bakayoko M, Sylla NF, Elsayed Ahmed Mohamed H, Jadvi K *et al.* Biosynthesis of TiO_2 nanoparticles by using natural extract of Citrus sinensis. Mater Today. 2021;36:349–356. https://doi.org/10.1016/j.matpr.2020.04.131.
42. Al-Hamoud K, Shaik MR, Khan M, Alkhathlan HZ, Adil SF, Kuniyil M *et al.* Pulicaria undulata extract-mediated eco-friendly preparation of TiO_2 nanoparticles for photocatalytic degradation of methylene blue and methyl orange. ACS omega. 2022;7(6):4812–4820. https://doi.org/10.1021/acsomega.1c05090.
43. Khoiriah K, Safni S, Syukri S, Gunlazuardi J. The operational parameters effect on photocatalytic degradation of diazinon using carbon and nitrogen modified TiO_2. Rasayan J Chem. 2020;13(3):1919–1925. http://dx.doi.org/10.31788/RJC.2020.1335743.
44. Atta ul Haq, Muhammad Saeed, Khan SG, Ibrahim M. Photocatalytic applications of titanium dioxide (TiO_2). in Titanium Dioxide - Advances and Applications. IntechOpen. 2022. https://doi.org/10.5772/intechopen.99598.
45. Akakuru OU, Iqbal ZM, Wu A. TiO_2 Nanoparticles: Properties and applications. In: Aiguo W, Ren W, editors. TiO_2 Nanoparticles: Applications in Nanobiotechnology and Nanomedicine. Wiley-VCH Verlag GmbH & Co. 2020. https://doi.org/10.1002/9783527825431.ch1.
46. Groeneveld I, Kanelli M, Ariese F, Bommel MRv. Parameters that affect the photodegradation of dyes and pigments in solution and on substrate – An overview. Dyes Pigm. 2023;210(110999):1–14. https://doi.org/10.1016/j.dyepig.2022.110999.
47. Kader S, Al-Mamun MR, Suhan MBK, Shuchi SB, Islam MS. Enhanced photodegradation of methyl orange dye under UV irradiation using MoO_3 and Ag doped TiO_2 photocatalysts. Environ Technol Innov. 2022;27(102476):1–15. https://doi.org/10.1016/j.eti.2022.102476.
48. Tang WZ, Zhang Z, An H, Quintana MO, Torres DF. TiO_2/UV photodegradation of azo dyes in aqueous solutions. Environ Technol. 2010;18(1):1–12. http://dx.doi.org/10.1080/09593330.1997.9618466.

التحلل الضوئي للحمض الأصفر 25 باستخدام مستخلص قرون البتايا بوساطة ثاني أكسيد التيتانيوم النانوي

أنتوني باتاهان أريتونانج[1]، رضا أودينا بوتري[2]، فيفي سيسكا[2]، محمد جهاد مادیابو[3]، خيريا خويريا[2]

[1] قسم الكيمياء، العلوم الطبيعية والرياضيات، جامعة تانجونجبورا، بونتياناك، إندونيسيا.
[2]مركز أبحاث الكيمياء، الوكالة الوطنية للبحث والابتكار، سيربونج، إندونيسيا.
[3] قسم الكيمياء التحليلية، بوليتكنيك بوجور، بوجور، إندونيسيا.

الخلاصة

تتمتع تقنية النانو بمزايا كبيرة مقارنة بالطرق التقليدية لتحلل الأصباغ. تم توليد جسيمات نانوية نباتية بعيدًا عن المواد الحيوية الأخرى. استخدم هذا العمل نهج هلام السول الأخضر لإعداد جسيمات نانوية من ثاني أكسيد التيتانيوم باستخدام مستخلص قشر البتايا (Parkia speciosa). تم تحليل ثاني أكسيد التيتانيوم الناتج بواسطة XRD وUV-DRS وFE-SEM وFTIR وRaman وzeta وتحليل حجم الجسيمات النانوية. تم إنتاج جسيمات نانوية من PP-TiO2 ذات طور أناتاز رباعي الزوايا وجسيمات كروية مستقرة وحجم جسيم صغير (16-22 نانومتر) بنجاح. عند تعرضها للأشعة فوق البنفسجية، أظهرت الجسيمات النانوية نشاطًا ضوئيًا قويًا، مما أدى إلى القضاء على الحمض الأصفر 25 في أقل من 120 دقيقة. يوضح هذا العمل خيارًا أخضرًا محتملًا لمعالجة مياه الصرف الصحي المستدامة استنادًا إلى جسيمات نانوية من ثاني أكسيد التيتانيوم.

الكلمات المفتاحية: الاستراتيجيات الخضراء، الجسيمات النانوية، البتايا، المحفز الضوئي، ثاني أكسيد التيتانيوم.